

Renal sympathetic nerve denervation using intraluminal ultrasound within a cooling balloon preserves the arterial wall and reduces sympathetic nerve activity

Atul Pathak^{1,2,3,6*}, MD, PhD; Leslie Coleman⁴, DVM, MS; Austin Roth⁴, MS; James Stanley⁴, MS; Lynn Bailey⁵, DVM, MS; Peter Markham⁵; Sebastian Ewen⁷, MD; Charlotte Morel^{1,2}, PharmD; Fabien Despas^{1,2,3}, PharmD, PhD; Benjamin Honton⁶, MD; Jean Michel Senard^{1,2,3}, MD, PhD; Jean Fajadet⁶, MD; Felix Mahfoud⁷, MD, PhD

1. National Institute of Health and Medical Research (INSERM) UMR-1048, Institute of Metabolic and Cardiovascular Diseases, Toulouse, France; 2. Toulouse University III - Paul Sabatier, Toulouse, France; 3. Clinical Pharmacology Department, University Hospital of Toulouse, Toulouse, France; 4. ReCor Medical, Palo Alto, CA, USA; 5. CBSET, Inc., Lexington, MA, USA; 6. Cardiovascular Department, Hypertension and Heart Failure Unit, Clinique Pasteur, Toulouse, France; 7. Klinik für Innere Medizin III, Universitätsklinikum des Saarlandes, Homburg/Saar, Germany

KEYWORDS

- catheter
- norepinephrine (NEPI)
- renal artery
- renal sympathetic denervation
- ultrasound

Abstract

Aims: Circumferential ablation of renal sympathetic nerves using catheter-based ultrasound energy was studied in a preclinical *in vivo* model. The aim was to investigate the benefit of cooling the arterial wall and the extent of renal nerve injury based on histopathology, and to correlate the injury with kidney norepinephrine levels.

Methods and results: Computer simulations of the ultrasound transducer within the cooling balloon demonstrated a circumferentially uniform heating profile. *In vivo* characterisation was performed in 10 normotensive pigs. Nine were treated bilaterally with ultrasound and survived for seven days (n=8) or were sacrificed acutely (n=1). Acutely, TTC staining of the renal arteries treated with ultrasound energy in the presence of cooling demonstrated viable tissue consistent with preservation of the arterial medial layer. Histological studies demonstrated no endothelial injury and minimal to no injury to the media of the renal arterial wall at seven days. Overall, circumferential nerve damage with up to 76% of nerve bundles affected within 7.5 mm of the arterial lumen was observed. Kidney norepinephrine (NEPI) levels were significantly reduced in all animals compared to a non-treated control animal (n=1) and correlated with the degree of nerve damage. A greater reduction in NEPI and a greater percentage of affected nerves was observed in arteries treated with two or three bilateral ultrasound emissions.

Conclusions: Catheter-based ultrasound delivered within a cooling balloon is effective at targeting the majority of the renal nerves circumferentially, resulting in significantly decreased kidney NEPI levels without damaging the arterial wall in a porcine model.

*Corresponding author: Department of Cardiovascular Medicine, Hypertension and Heart Failure Unit, Clinique Pasteur, 65 avenue de Lombez, 31076 Toulouse, France. E-mail: apathak@clinique-pasteur.com

Introduction

Catheter-based renal denervation (RDN) using radiofrequency energy is an approach to disrupt renal sympathetic nerve activity that can result in lowering blood pressure in patients with resistant hypertension¹⁻³. However, the treatment effect is highly variable and, in a relevant proportion of patients undergoing the procedure, blood pressure is not reduced sufficiently⁴. The neutral outcome of the recently published SYMPPLICITY HTN-3 study⁴, where a monopolar radiofrequency device has been used, underscores the considerable heterogeneity in individual responses and the potential limitations of mono-electrode radiofrequency (RF) ablation technology.

Catheter-based RDN is thought to cause partial depletion of the sympathetic innervation in the kidney; however, data have focused on devices delivering RF energy⁵. The PARADISE® Percutaneous Renal Denervation System (ReCor Medical Inc., Palo Alto, CA, USA) is a next-generation catheter-based device which has been designed to deliver ultrasound (U/S) energy to perform targeted circumferential ablation of renal efferent and afferent sympathetic nerves⁶. The catheter includes a cooling balloon to preserve the integrity of the renal arterial wall and near-field tissue and to position the U/S transducer accurately within the renal artery. The objective of this study was to evaluate the benefit/risk ratio of the cooling U/S-based balloon technology by analysis of nerve ablation effectiveness through norepinephrine (NEPI) measurements, and by the correlation of NEPI levels with histologic evidence of nerve ablation. Further, preservation of the renal artery was evaluated through histologic assessment of the renal arteries and surrounding tissues in arteries treated with one, two or three U/S emissions bilaterally.

Methods

DEVICE OVERVIEW

The PARADISE system consists of a single-use 6 Fr femoral delivery catheter and an automated, portable customised generator. The catheter consists of a through-lumen shaft with a cylindrical piezoelectric ceramic transducer located at the distal end of the catheter. The catheter has a distal balloon, which is pressurised by the generator to a range of 1.5-2.0 atm using sterile circulating water. The U/S transducer is centred within the balloon. The transducer converts electrical energy to acoustic energy, which is then delivered radially through the cooling balloon and into the renal artery. The pressurised balloon centres the U/S transducer within the artery, and the circulation of fluid serves as coolant to protect the endothelial and medial layers of the renal arterial wall. Each catheter has an embedded chip that communicates directly with the generator the specific power settings to be applied.

ULTRASOUND TRANSDUCER (COMPUTER SIMULATION OF ENERGY DELIVERED)

Computer simulations were developed to simulate use of the U/S transducer in tissue and to characterise the heat pattern generated when U/S energy is delivered through a cooling balloon. Computer models incorporated transducer properties, such as

driving frequency and input power, as well as convective cooling at the interface of the balloon and surrounding tissues. Simulations of transducer acoustic output and tissue heat transfer were accomplished using finite-element and finite-difference methods with rectangular mesh discretisation⁷. Finite-difference calculations for two-dimensional acoustic and thermal simulations were completed using MATLAB (MathWorks, Inc., Natick, MA, USA), while Multiphysics® finite element software (COMSOL, Inc., Burlington, MA, USA) was used to solve three-dimensional heat transfer problems. Finite element simulations used an approximated heat source to mimic ultrasound absorption heating, while the convective cooling at the vessel wall was approximated with a convective heat transfer coefficient of $5,000 \text{ W/m}^2 \cdot \text{K}$ ⁸.

STUDY DESIGN

The study enrolled 10 normotensive Yorkshire cross swine (*Sus scrofa*), of either sex, ranging from 74.8 to 89.0 kg. All procedures for this study were performed at CBSET, Inc. (Lexington, MA, USA) in compliance with the USDA Regulations and the Animal Welfare Act (9 CFR Parts one, two and three). The Guide for the Care and Use of Laboratory Animals was followed. The protocol for this study was reviewed and approved by the Institutional Animal Care and Use Committee (IACUC) of the test facility, which is accredited by the Association for Assessment and Accreditation of Laboratory Animal Care (AAALAC).

Ten animals were placed into two study groups (**Table 1**). Group A included eight animals treated with one (n=3), two (n=3), or three (n=2) U/S emissions in the proximal, mid, and/or distal regions of both renal arteries, and which survived for seven days. The kidneys were analysed for NEPI levels by HPLC-MS; the renal arteries along with associated nerves were assessed by histopathology. One additional animal served as a naïve control for the purposes of obtaining NEPI in an animal which did not undergo intervention. Group B included one animal treated with one U/S emission without concomitant cooling in the proximal portion of both renal arteries and one U/S treatment with concomitant cooling in the mid portion of both renal arteries. The animal was sacrificed immediately and the renal arteries stained with tetrazolium chloride (TTC) to evaluate the viability of the renal artery tissue immediately following energy delivery.

RENAL DENERVATION PROCEDURE AND FOLLOW-UP

All animals were treated with aspirin (650 mg PO) and clopidogrel (300 mg PO) 24 hours prior to the procedure. Animals were anaesthetised for the RDN procedure with Telazol® (4-6 mg/kg IM) followed by isoflurane anaesthesia by mask to facilitate endotracheal intubation. Animals were maintained on isoflurane anaesthesia for the duration of the procedure. Animals were prepared for aseptic surgery, and vascular access was obtained via the femoral artery percutaneously or vascular cutdown. An 8 Fr introducer sheath was placed, and intravenous heparin administered to achieve an activated clotting time (ACT) of >275 seconds. The right and left renal arteries of the pig were engaged using a 7 Fr RDC Launcher

Table 1. Study design.

Group number	Number of animals	Treatment	Treatment details	Necropsy time point	Analysis
A	8	Bilateral denervation of renal arteries with ultrasound	One 30 sec ultrasound emission – 2 arteries treated in proximal RA – 2 arteries treated in mid RA – 2 arteries treated in distal RA	Day 7	Renal artery histology and whole kidney norepinephrine analysis
			Two 30 sec ultrasound emissions – 2 arteries treated in prox/distal RA – 2 arteries treated in mid/distal RA – 2 arteries treated in prox/mid RA		
			Three 30 sec ultrasound emissions – 4 arteries treated in prox/mid/distal RA		
	1	None	None	n/a	Whole kidney norepinephrine analysis (NEPI control)
B	1	Bilateral denervation of renal arteries with ultrasound	30 sec ultrasound emission+cooling (mid artery)	Day 0	TTC staining
			30 sec ultrasound emission without cooling (proximal artery)		

*RA: renal artery

guiding catheter (Medtronic, Minneapolis, MN, USA). Prior to the RDN procedure, angiography of each renal artery was performed using Omnipaque 300. The length and diameter of the renal artery were measured to determine the appropriate size catheter for treatment. A 6 Fr catheter was introduced and positioned in the right or left renal artery via fluoroscopic guidance. Bilateral denervation was achieved by delivering ultrasound energy in up to three locations within each renal artery starting in a distal position then repositioning more proximally for sequential treatments. The animals were euthanised at day zero (Group B, n=1) or day seven (Group A, n=8; and the naïve control, n=1). All animals in Group A were treated post procedure with aspirin (81 mg PO) and clopidogrel (75 mg PO) daily. Clinical observations, including body condition scores (scale of 0-5 whereby 1=emaciated, 2=normal, 3=obese) and body weight (kg), were performed daily. Blood samples for clinical pathology were collected before treatment and prior to euthanasia. The renal arteries were perfused with Lactated Ringer's followed by 10% NBF and submitted for histopathology (Group A), or perfused with TTC solution (Group B). Whole kidneys were flash frozen in 4 gm aliquots for NEPI measurements (Group A). Observations of gross macroscopic findings in surrounding non-target tissues were recorded and tissues with injury were submitted for histologic examination.

TTC STAINING

Staining with TTC was used to assess the viability of the renal arterial tissue acutely post RDN. The technique utilised was adapted from techniques commonly used to assess the size of acute myocardial infarcts in preclinical models^{9,10}. Briefly, renal arteries in Group B were perfused with TTC solution *in situ*, harvested, and then immersed in TTC stain solution at 37°C with no exposure to light until a colour change was observed. Arteries were bisected longitudinally to allow for visualisation of the luminal surface. Viable tissue stains red whereas non-viable tissue (regions of

infarct) appears white in the presence of denatured or degraded dehydrogenase enzymes that can no longer react with the tetrazolium salt.

HISTOLOGY

Renal arteries with surrounding tissue were cut into five sections along the length of the artery. A representative slide from each section was evaluated by light microscopy. Semi-quantitative scoring of the renal arterial response was performed to evaluate the impact of the therapy on the endothelium, medial layer, and adventitia. The percentage of endothelial cell coverage by quadrant was determined (zero=absent, one=<25% coverage, two=25-75% coverage, three=>75% coverage, four=100% confluence of luminal surface). Medial injury was scored (zero=no injury, one=disruption of the IEL, two=disruption of the tunica media, three=disruption of the EEL). Inflammation in the medial and adventitial layers was scored (zero=none, one=mild, two=moderate, three=severe). Semi-quantitative scoring of nerve damage was performed using a scale of zero to three (zero=absent, one=minimal injury, two=moderate injury, three=severe injury). Quantification of damaged nerves circumferentially was performed to determine the percentage of ablated nerves surrounding the renal artery. All assessments were performed by a single investigator. Comparisons were made among animals treated with one, two or three U/S emissions bilaterally.

WHOLE KIDNEY NOREPINEPHRINE (HPLC-MS ASSAY)

Six 4 gm aliquots were collected from each kidney and flash frozen in liquid nitrogen for subsequent analysis for NEPI content. NEPI levels were measured by high performance liquid chromatography – mass spectrometry (HPLC-MS/MS) using a non-GLP Research Grade 3 Assay through reductive ethylation to norepinephrine-d6 and epinephrine-d3 as IS, on API-5500 Q-trap using positive ion TurboIon spray. Three of the six 4 gm aliquots were analysed (three

aliquots were kept in reserve), and the data averaged to obtain a NEPI level per kidney. NEPI levels were reported as ng/g renal tissue. The percentage reduction of NEPI compared to an untreated control was determined. Comparisons of the mean NEPI level, and percent reduction of NEPI, by number of bilateral treatment emissions were performed. Additionally, the correlation between mean NEPI level by number of treatment emissions and percentage of ablated nerves (determined by histology) was assessed.

STATISTICAL ANALYSIS

Linear regression repeated measures models (fit via generalised estimating equations, with an exchangeable working correlation structure) were used to account for multiple measurements per subject. Bonferroni adjustments to nominal p-values were used to control the type I error rate for the pairwise contrasts among groups.

Results

COMPUTER SIMULATION OF ACOUSTIC ENERGY AND THERMAL PROFILE

Simulated use of the U/S transducer within a cooling balloon demonstrated a distinct temperature profile. The shape of the temperature profile is defined by the combination of the beam energy profile, heat conduction in the tissue, and the cooling effect accomplished by the balloon at the surface of the arterial wall. The 3D temperature profile demonstrates the formation of a circumferentially uniform toroidal lesion with a spared cooled zone (Figure 1).

IN VIVO STUDY

The device was used successfully in all nine animals. All animals survived the expected in-life phase of the study. There were no changes in body weight or body condition score between baseline and day seven. Clinical pathology results (complete blood count and serum chemistries including creatinine and electrolytes) were unchanged between baseline and day seven.

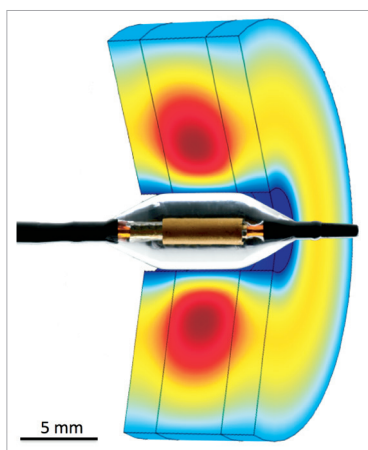


Figure 1. Predicted 3D tissue temperature profile associated with the PARADISE catheter. The temperature map demonstrates a preserved cooled region (blue) adjacent to the balloon and a uniform cylindrical heat lesion beyond the cooled region (orange-red).

ACUTE ASSESSMENT OF VIABLE AND NON-VIABLE TISSUE AFTER TREATMENT OF AREA WITH TTC STAIN (GROUP B)

Acute TTC staining of the renal arteries allowed for distinct delineation of viable versus non-viable arterial tissue following treatment with either U/S emission with cooling (mid artery) or U/S emission without concomitant cooling (proximal artery). The luminal surface of the adjacent aorta and bilateral renal arteries exhibited a deep red appearance which demonstrated the uptake of TTC by viable cells in the mid portion of both renal arteries, whereas the proximal portion of both renal arteries had blanched, circumferential regions indicative of non-viable tissue (Figure 2).

RENAL ARTERY HISTOLOGY, SEVEN DAYS POST ULTRASOUND TREATMENT

Sections of renal arteries were analysed to assess the distance of the renal nerves from the luminal-intima border and accordingly the extent of denervation. The renal arterial wall as well as the immediately adjacent adventitia was generally spared. A semi-quantitative assessment of medial injury, medial inflammation, and adventitial inflammation demonstrated that there was minimal to no medial injury or inflammation observed regardless of the number of treatment emissions. Adventitial inflammation ranged from minimal to moderate depending on the number of treatment emissions delivered along the length of the artery. There were no thrombi, dissections, stenoses, aneurysms, mural perforations or lacerations, haematomas or other device-related pathologies. The luminal surface of the renal artery was almost completely endothelialised after one, two, and three ultrasound emissions (Figure 3).

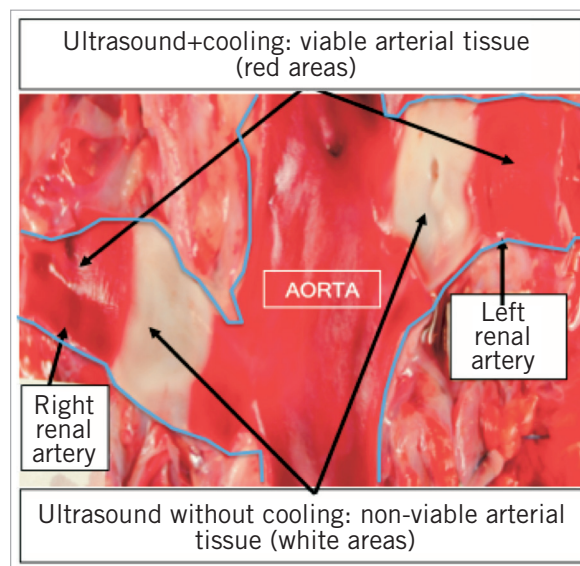


Figure 2. Triphenyltetrazolium chloride (TTC) stained macroscopic images. Macroscopic image of porcine aorta with bifurcating left and right renal arteries. White tissue represents non-viable renal artery following ablation with ultrasound in the absence of cooling demonstrating a transmural burn. Red tissue at the mid level of both renal arteries represents viable arterial tissue following ablation with ultrasound and cooling.

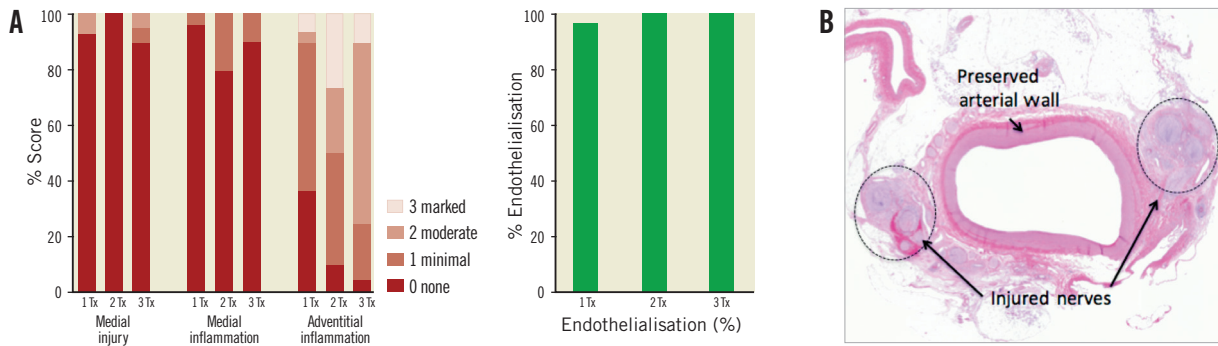


Figure 3. Histopathology of the renal artery and surrounding nerves seven days post treatment with ultrasound and cooling. *A)* Semi-quantitative scoring of the renal artery histopathology delineated by number of emissions per artery. *B)* Photomicrograph of a histologic cross-section of a porcine renal artery seven days post treatment with ultrasound renal denervation characterised by arterial wall preservation due to cooling and renal nerve necrosis in the ablation zone haematoxylin and eosin stain.

Effects on adjacent structures, including focal psoas muscle necrosis, focal transmural necrosis of colon, and injury to the ureter were occasionally observed when the U/S ablation area exceeded 7.5 mm.

In the porcine model in this study (n=8 normotensive pigs), the majority of renal nerves were located within 7.5 mm of the arterial luminal surface. An in-depth analysis of the distribution of nerves, and the magnitude and location of injured nerves post U/S ablation was performed in six animals which received either one or two bilateral U/S emissions. Animals with three emissions were not included in this analysis to ensure that two discrete thermal ablation areas could be analysed. Nerve distribution along the renal artery in these animals was characterised as, on average, 33% located within 2.5 mm of the luminal surface, 36% located between 2.5 and 5 mm of the luminal

surface, 21% located within 5 and 7.5 mm of the luminal surface, and 10% beyond 7.5 mm (**Figure 4A**). The majority of injured nerves were located circumferentially within 7.5 mm of the arterial lumen and many of these nerve bundles were characterised by marked degenerative change accompanied by necrosis (**Figure 4B**). Increasing the number of treatments along the length of the artery positively correlated with an increase in the number of nerves directly affected. A statistically significant difference in the number of affected nerves was observed in one bilateral U/S emission per artery (44% injured) compared to two (76% injured) (p=0.004) or three bilateral U/S emissions per artery (76% injured) (p=0.001). No significant difference in the percentage of nerves ablated was observed between two and three U/S emissions per artery (p=1.0) (**Figure 5**).

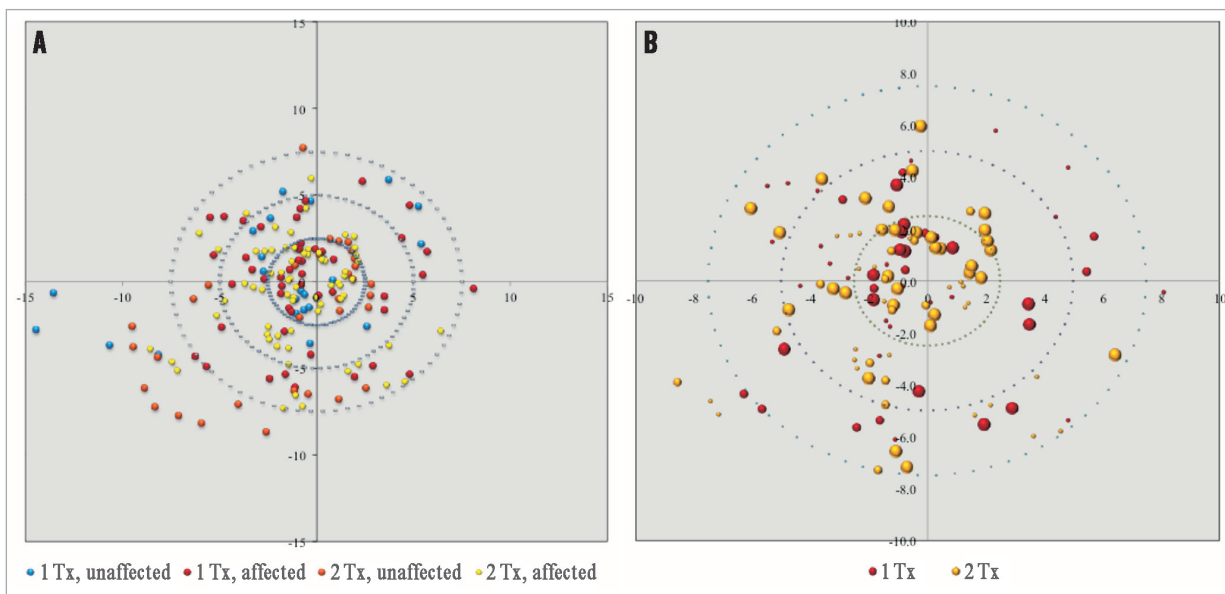


Figure 4. Renal nerve distribution in porcine model and effectiveness of nerve ablation with U/S catheter-based RDN. *A)* Distribution of renal nerves, mm from the arterial lumen. Red and yellow dots represent ablated nerves following one or two bilateral U/S emissions, respectively. Blue and orange dots represent non-ablated nerves. *B)* Location of ablated nerves (mm from the arterial lumen) following one or two bilateral U/S emissions. The size of the dot represents the extent of injury whereby the larger size is consistent with moderate-severe nerve injury. Note: data represent cumulative injury along the length of the artery irrespective of orientation.

WHOLE KIDNEY NOREPINEPHRINE LEVEL

There was a correlation of kidney NEPI with the number of bilateral U/S treatments per artery. An increase in the number of treatments per artery lowered the NEPI levels incrementally in a linear fashion ($R^2=0.903$), resulting in mean renal NEPI reductions of 55%, 89% and 97% with one, two, and three U/S emissions per artery, respectively (Figure 5). The reduction in NEPI concentrations also correlated significantly with the percentage of sympathetic nerves ablated ($p<0.0001$). As shown, two and three U/S emissions per renal artery ablated 76% of renal sympathetic nerves along the length of the artery, whereas a single treatment resulted in the ablation of 44% of afferent and efferent renal nerve fibres.

Discussion

Renal denervation has been shown to reduce blood pressure and sympathetic activity in certain but not in all patients with uncontrolled hypertension¹¹⁻¹³. Insufficient ablation of renal sympathetic nerves has been discussed as a potential reason for non-response to treatment^{14,15}. Herein, we investigated in a preclinical model the effectiveness of a next-generation catheter-based system using U/S to ablate the renal sympathetic nerves circumferentially.

Computer modelling of the heat pattern generated by the transducer was utilised to predict the size and geometry of the thermal lesion generated *in vivo*. Therapeutic ultrasound energy consists of high-frequency sound waves (i.e., rapid mechanical oscillations) that generate frictional heating in soft tissue. Peak temperature associated with U/S energy is greatest nearest the transducer. As the acoustic energy travels through the tissue, the temperature decreases due to absorption of the energy. The computer model demonstrated that the cooling balloon shifts the peak temperature generated by the transducer into the peri-arterial tissue (1 mm cooled zone measured *in vivo*) by cooling the tissue nearest the transducer. The model further demonstrated that a consistent lesion characterised by controlled toroidal geometry is created through use of a cylindrical transducer

centred within a cooling balloon. This observation was confirmed *in vivo* by acute TTC data and by seven-day histopathology wherein both demonstrated preservation of the arterial wall associated with the cooling balloon. The cooling balloon therefore has a vasculoprotective effect without reducing nerve ablation effectiveness. Gross pathology and histological assessment of vascular lesions show that all layers of the arterial wall have been preserved despite an increase in the number of U/S applications.

This study demonstrated that bilateral denervation of the kidneys with U/S resulted in a marked reduction in kidney norepinephrine (NEPI) levels which correlated with the percentage of nerves ablated as determined by histology, indicating the effectiveness of the device. One, two, and three U/S emissions bilaterally in the renal arteries reduced NEPI levels compared to a control by 55%, 89%, and 97%, respectively, which translated into circumferential ablation of nerves by 44%, 76%, and 76%, respectively. These data demonstrate a significant difference between one and two emissions ($p=0.004$) bilaterally; however, no difference was observed between two and three emissions bilaterally ($p=1.0$). Furthermore, the data demonstrated that nerves were ablated in a largely circumferential pattern at depths ranging from 1-7.5 mm, and occasionally extending beyond 7.5 mm, thereby targeting the vast majority of the renal nerves, which may be important given the distribution of renal sympathetic nerves across the renal artery¹⁶.

The kidney NEPI level decrease appears to be related to a dose cumulative effect since above two circumferential ablations the decrease was not statistically significant. Moreover, the decrease seems to be maximal after two circumferential ablations, probably due to near complete to complete severance of multiple nerve bundles running along the renal artery at varying depths. Although this study was not designed specifically to quantify the level of renal denervation, the reduction in renal NEPI levels observed corresponds well with the histological analysis of renal nerve injury. There was a significant correlation between renal tissue NEPI and nerve injury ($p<0.0001$).

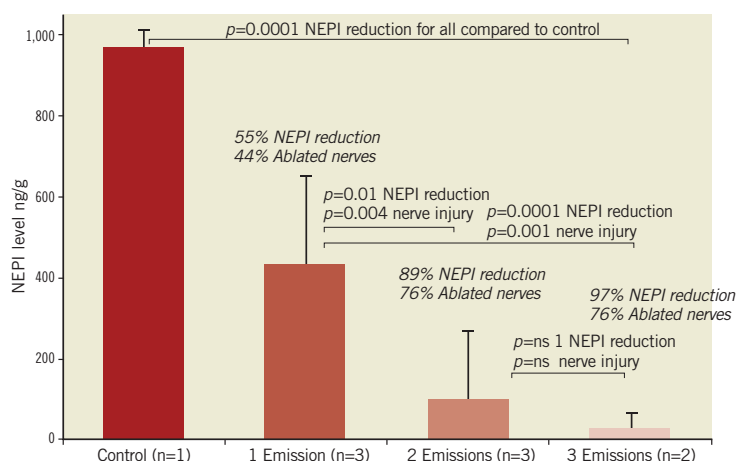


Figure 5. Percent NEPI reduction and percent ablated nerves based on the number of bilateral ultrasound emissions. A) A statistically significant difference was observed in NEPI reduction following one, two or three U/S emissions compared to control. A significant difference was observed between one bilateral U/S emission and two or three emissions. However, there was no difference between two and three bilateral U/S emissions, suggesting a maximum effect of treatment with two emissions. Data presented as mean \pm SD.

This study demonstrated that the majority of the renal nerves in the porcine model are located within 7.5 mm of the arterial lumen. These findings correlate well with the anatomical distribution of nerves in humans wherein the majority are located within 8 mm of the arterial lumen¹⁶. Ultrasound energy is highly controllable and can be delivered to reach target depths at ablative temperature, leading to a reduction of renal tissue NEPI content. Herein, NEPI levels were decreased by 90% after U/S ablation of the renal nerves with two or three bilateral emissions. The ability to deliver ablative temperatures to injure nerves at depth is a differentiating feature of ultrasound as compared to RF ablation. RF ablation relies on direct tissue contact with the RF electrode to induce thermal damage and relies on thermal conduction to target nerves residing away from the arterial wall. As such, catheter-based RDN utilising RF energy has a relatively limited depth of penetration¹⁷. Recently, Vink et al published a case report on the histopathology findings 12 days post RF RDN in a patient with resistant hypertension¹⁸. They reported intimal to peri-adventitial damage in a wedge shape extending to 2 mm from the arterial lumen with incomplete and variable damage of the nerve bundles. Ultrasound does not require direct tissue contact to heat surrounding tissues, which allows the incorporation of a cooling balloon to protect the endothelial and medial layers of the arterial wall. Further, ultrasound energy propagates into tissues, depositing energy in a predictable pattern. In this study, occasional damage to adjacent non-target organs was observed. As U/S energy is highly controllable, the thermal profile associated with this system has been adjusted to create consistently an ablation area that does not exceed 7.5 mm to ensure that maximal nerve injury is achieved without damaging retroperitoneal organs, which was occasionally observed when the U/S ablation area exceeded 7.5 mm¹⁹.

The SYMPLICITY HTN-3 data demonstrated that catheter-based RDN using RF energy is safe; however, the primary efficacy endpoint of the trial was not met⁴. There is an ongoing discussion regarding the reasons why the trial failed to meet its primary endpoint, including technology and procedural issues²⁰. One major limitation of all current technologies is the lack of procedural feedback regarding ablation of nerves. Preclinical models allow a unique assessment of the effectiveness of renal denervation in that the direct effect on nerves can be assessed by histopathologic evaluation. Translation of preclinical data into clinical therefore becomes paramount²¹. In this study we demonstrated a significant reduction in NEPI which correlated with the percentage of nerves affected. Further, we demonstrated that nerves were ablated circumferentially, and the arterial wall was consistently spared. Clinical trials are needed to confirm the favourable efficacy and safety profile of the system.

Limitations

These data were generated in normotensive pigs. The clinical implications of preclinical findings in hypertensive patients are therefore uncertain. Further, the NEPI reductions were compared to one control animal; there is known variability of baseline NEPI levels in pigs. Moreover, NEPI levels were assessed globally in the kidney tissue and not specifically at the level of vessels or synaptic cleft. The

correlation of reductions in NEPI in a porcine model and the observation of marked nerve injury with clinical benefit such as BP lowering in humans is not known. Preclinical work is ongoing to understand the impact of delivering ultrasound energy at locations of atherosclerosis, as are clinical studies with the PARADISE RDN System. The translation of preclinical results into clinical outcomes can only be determined as greater clinical experience is gained with these systems.

Conclusion

Catheter-based ultrasound ablation of the renal nerves reduces sympathetic nerve fibres and their activity without significantly compromising short-term vascular integrity. The data from this study also indicate that a minimum of two circumferential lesions per artery reduces NEPI content by >90%. The ultrasound RDN device used in our study is able to affect renal sympathetic fibres significantly, with injury observed along the renal artery in 76% of the nerves with two bilateral ultrasound emissions.

Impact on daily practice

Renal denervation has been developed to reduce sympathetic activity in conditions such as hypertension and heart failure. This study demonstrated that bilateral denervation of the kidneys with a device combining catheter-based ultrasound delivery within a cooling balloon is effective at targeting the majority of the renal nerves circumferentially. Renal denervation based on this approach resulted in significantly decreased kidney NEPI levels which correlated with the percentage of nerves ablated. Histological assessment showed that renal denervation was not damaging the arterial wall in this porcine model. Translation of these preclinical data into clinical therefore becomes paramount. These data suggest that this approach is effective in reducing sympathetic activity and safe for the arterial wall. Clinical trials are ongoing to confirm these observations.

Acknowledgements

The authors would like to thank CBSET, Inc., for performing the *in vivo* studies, and all associated bioanalytical work, TTC staining of the arteries, and histopathologic assessment of the renal arteries and nerves.

Funding

This study was sponsored by ReCor Medical, Inc.

Conflict of interest statement

F. Mahfoud and S. Ewen are supported by Deutsche Hochdruckliga und Deutsche Gesellschaft für Kardiologie. F. Mahfoud has received research grants, speaker's honoraria and/or consultancy fees from Medtronic, and St. Jude. A. Pathak has received research grants, speaker's honoraria and/or consultancy fees from Medtronic, Boston Scientific, ReCor Medical, and St. Jude Medical. L. Coleman and A. Roth are employees of ReCor Medical. The other authors have no conflicts of interest to declare.

References

1. Krum H, Schlaich M, Whitbourn R, Sobotka PA, Sadowski J, Bartus K, Kapelak B, Walton A, Sievert H, Thambar S, Abraham WT, Esler M. Catheter-based renal sympathetic denervation for resistant hypertension: a multicentre safety and proof-of-principle cohort study. *Lancet*. 2009;373:1275-81.
2. Esler MD, Krum H, Schlaich M, Schmieder RE, Böhm M, Sobotka PA. Renal sympathetic denervation for treatment of drug-resistant hypertension: one-year results from the Symplicity HTN-2 randomized, controlled trial. *Circulation*. 2012;126: 2976-82.
3. Schlaich MP, Schmieder RE, Bakris G, Blankestijn PJ, Bohm M, Campese VM, Francis DP, Grassi G, Hering D, Katholi R, Kjeldsen S, Krum H, Mahfoud F, Mancia G, Messerli FH, Narkiewicz K, Parati G, Rocha-Singh KJ, Ruilope LM, Rump LC, Sica DA, Sobotka PA, Tsioufis C, Vonend O, Weber MA, Williams B, Zeller T, Esler MD. International expert consensus statement: Percutaneous transluminal renal denervation for the treatment of resistant hypertension. *J Am Coll Cardiol*. 2013;62:2031-45.
4. Bhatt DL, Kandzari DE, O'Neill WW, D'Agostino R, Flack JM, Katzen BT, Leon MB, Liu M, Mauri L, Negoita M, Cohen SA, Oparil S, Rocha-Singh K, Townsend RR, Bakris GL; SYMPPLICITY HTN-3 Investigators. A controlled trial of renal denervation for resistant hypertension. *N Engl J Med*. 2014;370: 1393-401.
5. Tsioufis C, Mahfoud F, Mancia G, Redon J, Damascelli B, Zeller T, Schmieder RE. What the interventionalist should know about renal denervation in hypertensive patients: a position paper by the ESH WG on the interventional treatment of hypertension. *EuroIntervention*. 2014;9:1027-35.
6. Mabin T, Sapoval M, Cabane V, Stemmet J, Iyer M. First experience with endovascular ultrasound renal denervation for the treatment of resistant hypertension. *EuroIntervention*. 2012;8:57-61.
7. Minkowycz WJ, Sparrow EM, Abraham JP. Numerical Models of Blood Flow Effects in Biological Tissues. *Advances in Numerical Heat Transfer*. Volume 3. CRC Press; 2009;3:42.
8. dos Santos I, Haemmerich D, Pinheiro C, da Rocha AF. Effect of variable heat transfer coefficient on tissue temperature next to a large vessel during radiofrequency tumor ablation. *Bio Med Eng OnLine*. 2008;7:21.
9. Nachlas M, Schnitka T. Macroscopic identification of early myocardial infarcts by alterations in dehydrogenase activity. *Am J Pathol*. 1963;42:379-406.
10. Fishbein MC, Meerbaum S, Rit J, Londo U, Kanmatsuse K, Mercier JC, Corday E, Ganz W. Early phase acute myocardial infarct size quantification: validation of the triphenyl tetrazolium chloride tissue enzyme staining technique. *Am Heart J*. 1981;101:593-600.
11. Mahfoud F, Lüscher TF, Andersson B, Baumgartner I, Cifkova R, Dimario C, Doevendans P, Fagard R, Fajadet J, Komajda M, Lefèvre T, Lotan C, Sievert H, Volpe M, Widimsky P, Wijns W, Williams B, Windecker S, Witkowski A, Zeller T, Böhm M; European Society of Cardiology. Expert consensus document from the European Society of Cardiology on catheter-based renal denervation. *Eur Heart J*. 2013;34:2149-57.
12. Mahfoud F, Ukena C, Schmieder RE, Cremers B, Rump LC, Vonend O, Weil J, Schmidt M, Hoppe UC, Zeller T, Bauer A, Ott C, Blessing E, Sobotka PA, Krum H, Schlaich M, Esler M, Böhm M. Ambulatory blood pressure changes after renal sympathetic denervation in patients with resistant hypertension. *Circulation*. 2013; 128:132-40.
13. Schmieder RE, Redon J, Grassi G, Kjeldsen SE, Mancia G, Narkiewicz K, Parati G, Ruilope L, van de Borne P, Tsioufis C; European Society of Hypertension. Updated ESH position paper on interventional therapy of resistant hypertension. *EuroIntervention*. 2013;9 Suppl R:R58-66.
14. Ukena C, Cremers B, Ewen S, Bohm M, Mahfoud F. Response and non-response to renal denervation: who is the ideal candidate? *EuroIntervention*. 2013;9 Suppl R:R54-7.
15. Mahfoud F, Edelman ER, Bohm M. Catheter-based renal denervation is no simple matter: lessons to be learned from our anatomy? *J Am Coll Cardiol*. 2014;64:644-6.
16. Sakakura K, Ladich E, Cheng Q, Otsuka F, Yahagi K, Fowler D, Kolodgie F, Virmani R, Joner M. Anatomical assessment of sympathetic peri-arterial renal nerves in man. *J Am Coll Cardiol*. 2014;64:635-43.
17. Henegar JR, Zhang Y, Rama RD, Hata C, Hall ME, Hall JE. Catheter-based radiofrequency renal denervation lowers blood pressure in obese hypertensive dogs. *Am J Hypertens*. 2014;27:1285-92.
18. Vink EE, Goldschmeding R, Vink A, Weggemans C, Bleijs RL, Blankestijn PJ. Limited destruction of renal nerves after catheter-based renal denervation: results of a human case study. *Nephrol Dial Transplant*. 2014;29:1608-10.
19. Sakakura K, Roth A, Ladich E, Shen K, Coleman L, Joner M, Virmani R. Controlled circumferential renal sympathetic denervation with preservation of the renal arterial wall using intraluminal ultrasound: a next-generation approach for treating sympathetic overactivity. *EuroIntervention*. 2015;10:1230-8.
20. Kandzari DE, Bhatt DL, Brar S, Devireddy CM, Esler M, Fahy M, Flack JM, Katzen BT, Lea J, Lee DP, Leon MB, Ma A, Massaro J, Mauri L, Oparil S, O'Neill WW, Patel MR, Rocha-Singh K, Sobotka PA, Svetkey L, Townsend RR, Bakris GL. Predictors of blood pressure response in the SYMPPLICITY HTN-3 trial. *Eur Heart J*. 2015;36:219-27.
21. Mahfoud F, Böhm M, Azizi M, Pathak A, Durand Zaleski I, Ewen S, Tsioufis K, Andersson B, Blankestijn PJ, Burnier M, Chatellier G, Gafoor S, Grassi G, Joner M, Kjeldsen SE, Lüscher TF, Lobo MD, Lotan C, Parati G, Redon J, Ruilope L, Sudano I, Ukena C, van Leeuwen E, Volpe M, Windecker S, Witkowski A, Wijns W, Zeller T, Schmieder RE. Proceedings from the European clinical consensus conference for renal denervation: considerations on future clinical trial design. *Eur Heart J*. 2015 May 18. [Epub ahead of print].